Magnetic and magnetoelastic properties of $TmPO_4$



1996 J. Phys.: Condens. Matter 8 7967

(http://iopscience.iop.org/0953-8984/8/42/015)

J. Phys.: Condens. Matter **8** (1996) 7967–7980. Printed in the UK

# Magnetic and magnetoelastic properties of $TmPO_4$

P Morin†, J Rouchy† and Z Kazei‡

† Laboratoire Louis-Néel, CNRS, 166X, 38042, Grenoble Cédex, France
‡ Laboratory for Magnetism, Physics Department, Moscow State University, 119899, Moscow, Russia

Received 10 May 1996

**Abstract.** The rare-earth oxide compound $TmPO_4$ (tetragonal zircon structure) is investigated using the extended susceptibility formalism, which considers at any temperature all of the features of the crystalline electric field within the ground-state multiplet in the joint analysis of the magnetic, magnetoelastic and elastic properties. The magnetoelastic coefficients are determined from third-order magnetic susceptibility, parastriction and elastic constant measurements for the different symmetry modes. The dominant magnetoelastic coupling is associated with the orthorhombic $\delta$-symmetry; however, tetragonal and symmetry-lowering modes are also observed to give rise to noticeable effects, in particular in the thermal expansion. The close coherency between the magnetoelastic coefficients in $TmPO_4$ and $TbPO_4$ is then emphasized: the tetragonal magnetoelastic coefficients are sizeable and all of the magnetoelastic couplings keep the same sign and order of magnitude in the two phosphates. This coherency appears to be valid throughout the large family of rare-earth zircons. Through these two examples, the occurrence of a quadrupolar ordering is then discussed as being governed by the crystalline electric field, and the role of undercritical quadrupolar interactions is emphasized in $TmPO_4$.

## 1. Introduction

The study of magnetoelastic properties soared in popularity in the seventies for the dielectric compounds, and rare-earth (R) orthophosphates and orthovanadates are now considered as archetypes for the Jahn–Teller (JT) coupling (Gehring and Gehring 1975). Several of them ($DyVO_4$, $TbVO_4$, $TmVO_4$, $TbPO_4$) exhibit a spontaneous tetragonal–orthorhombic transition. Depending on the nature of the low-lying levels of the R ion, one can observe the change from the pure JT effect for an isolated non-Kramers doublet in $TmVO_4$ to a pseudo-JT effect for two close Kramers doublets in $DyVO_4$ or to a JT effect at an excited level for a singlet–doublet–singlet system in $TbVO_4$. The subject has recently received a new swell of interest in relation to structural phase transitions in high-temperature superconductors, manganites and fullerenes (Clougherty *et al* 1989, Schluter *et al* 1992).

Large magnetoelastic couplings are also present in R intermetallics and compete with the magnetic interactions. This coexistence has made necessary the development of microscopic models considering both types of interaction (Morin and Schmitt 1990). In particular a susceptibility formalism was developed in order to study separately each of the different magnetoelastic couplings and not only the dominant one, when strong enough to drive a structural transition. This approach considers all of the features of the crystalline electric field (CEF) in the ground-state multiplet. Unlike the case of pseudo-spin models, which have to be adapted to the compound under consideration, this approach allows one to achieve a general understanding of the magnetic and magnetoelastic properties for an entire family

0953-8984/96/427967+14$19.50  

of compounds. It has succeeded in explaining properties for very different situations such as in $TmAg_2$, a tetragonal compound with quadrupolar ordering (Morin and Rouchy 1993), as well as in NdZn, a cubic antiferromagnet, where the non-collinear magnetic structures are stabilized by (negative) antiferroquadrupolar interactions (Amara *et al* 1995). Among R insulators, it was applied to $TbPO_4$ (Morin *et al* 1994) and $HoVO_4$ (Morin *et al* 1995).

Among the R zircons, $TmPO_4$ belongs to the family of so-called four-level systems; the low-lying electronic states are two singlets at 0 and 110 K with a non-Kramers doublet at about 44 K (Knoll 1971). The behaviour of such systems is known to be determined by the balance between the strength of the JT correlations and the energy gap between the ground-state singlet and the doublet (Elliott *et al* 1972). Unlike those for $TbVO_4$, the JT interactions in $TmPO_4$ are not large enough to drive a structural transition, but remain close to criticality. A slight change of the wave functions and level spacings may stimulate the quadrupolar ordering, as predicted by Vekhter *et al* (1987), in the presence of an external magnetic field.

The JT interaction of $B_{2g}$ symmetry is dominant in $TmPO_4$. A large magnetoelastic contribution for the $C_{66}$ elastic mode was observed by Harley and Manning (1978), which drives a softening of about 85% at around 20 K. This strong, but non-zero dip in the temperature dependence of $C_{66}$ indicates that $TmPO_4$ does not undergo a spontaneous quadrupolar ordering, but remains undercritical. Additional evidence has also been obtained such as an anomalous field dependence of the magnetic moment along the [1 1 0] axis, characterized by an inflexion point in the magnetization curve (Ioffe *et al* 1981) or a substantial increase of the magnetostriction along the [1 1 0] axis (Bondar' *et al* 1988). However, there is no general approach which coherently explains all of the properties; for this, the susceptibility formalism may be a powerful tool. Therefore, after briefly recalling this method, we successively present the CEF, magnetic and magnetoelastic properties. A comparison with $TbPO_4$ is given in the discussion.

## 2. Formalism

The magnetic properties of the 4f shell are described with the usual Hamiltonian using the equivalent-operator method (Stevens 1952) and the mean-field approximation. It includes the CEF term, one- and two-ion couplings for both the magnetic and quadrupolar couplings, and the elastic energy (Morin *et al* 1988). The CEF term is written within a system of $x$-, $y$-, $z$-axes parallel to the [1 0 0], [0 1 0] and [0 0 1] directions of the lattice cell, respectively:

$$\mathcal{H}_{CEF} = \alpha_J V_2^0 O_2^0 + \beta_J (V_4^0 O_4^0 + V_4^4 O_4^4) + \gamma_J (V_6^0 O_6^0 + V_6^4 O_6^4). \tag{1}$$

The $O_l^m$ are the Stevens operators, $\alpha_J, \beta_J, \gamma_J$ the Stevens coefficients, and $V_l^m$ the CEF parameters. The magnetic terms are the Zeeman coupling to the applied magnetic field, $\boldsymbol{H}$, corrected for demagnetizing effects and the Heisenberg-type bilinear interactions. Only magnetoelastic contributions linear in strain and restricted to second-rank terms are considered here. They can be written in symmetrized notation as (du Trémolet de Lacheisserie 1970)

$$\mathcal{H}_{ME} = -(B^{\alpha 1}\varepsilon^{\alpha 1} + B^{\alpha 2}\varepsilon^{\alpha 2}) O_2^0 - B^{\gamma}\varepsilon^{\gamma} O_2^2 - B^{\delta}\varepsilon^{\delta} P_{xy} - B^{\varepsilon}(\varepsilon_1^{\varepsilon} P_{zx} + \varepsilon_2^{\varepsilon} P_{yz}). \tag{2}$$

The $B^{\mu}$ are the magnetoelastic coefficients, which are temperature independent. The related elastic energy is

$$E_{el} = \tfrac{1}{2} C_0^{\alpha 1} (\varepsilon^{\alpha 1})^2 + C_0^{\alpha 12} \varepsilon^{\alpha 1} \varepsilon^{\alpha 2} + \tfrac{1}{2} C_0^{\alpha 2} (\varepsilon^{\alpha 2})^2 + \tfrac{1}{2} C_0^{\gamma} (\varepsilon^{\gamma})^2 + \tfrac{1}{2} C_0^{\delta} (\varepsilon^{\delta})^2 + \tfrac{1}{2} C_0^{\varepsilon} [(\varepsilon^{\varepsilon 1})^2 + (\varepsilon^{\varepsilon 2})^2]. \tag{3}$$

The strains $\varepsilon^\mu$ and the lattice background elastic constants $C_0^\mu$ are expressed in Morin *et al* (1988) in terms of $\mu = \gamma, \delta, \varepsilon$ (the present terms $\alpha, \gamma, \delta$ and $\varepsilon$ correspond to the A, $B_{1g}$, $B_{2g}$ and E often used in the R zircon literature). The two-ion quadrupolar terms are written as

$$\mathcal{H}_Q = -K^\alpha \langle O_2^0 \rangle O_2^0 - K^\gamma \langle O_2^2 \rangle O_2^2 - K^\delta \langle P_{xy} \rangle P_{xy} - K^\varepsilon [\langle P_{yz} \rangle P_{yz} + \langle P_{zx} \rangle P_{zx}]. \tag{4}$$

Minimizing the free energy with respect to the strains gives the equilibrium strains as functions of the expectation values of the corresponding quadrupolar operators. Replacing these $\varepsilon^\mu$ makes equation (2) indistinguishable from equation (4) and leads to the total quadrupolar coefficients

$$G^\mu = \frac{(B^\mu)^2}{C_0^\mu} + K^\mu \tag{5}$$

and

$$G^\alpha = \frac{(B^{\alpha 1})^2 C_0^{\alpha 2} - 2B^{\alpha 1} B^{\alpha 2} C_0^{\alpha 12} + (B^{\alpha 2})^2 C_0^{\alpha 1}}{C_0^{\alpha 1} C_0^{\alpha 2} - (C_0^{\alpha 12})^2} + K^\alpha. \tag{5'}$$

This quadrupolar Hamiltonian is obviously reminiscent of the JT pseudo-spin model (Gehring and Gehring 1975, Melcher 1976). In the presence of only acoustic phonon exchange, the pair interaction coefficient $K^\mu$ is negative and a value of $-\frac{1}{3}$ is expected for the ratio of $K^\mu$ to the magnetoelastic contribution to $G^\mu$, $G^\mu_{ME} = (B^\mu)^2/C_0^\mu$, as observed in $TmVO_4$.

In the presence of small external stresses, perturbation theory can be applied very fruitfully to the disordered phase. It is then possible to obtain analytical expressions for the free energy associated with each of the five symmetry-lowering modes and then to describe the corresponding couplings. For example the third-order magnetic susceptibility, i.e. the $H^3$-term in the field expansion of the magnetization, reads

$$\chi_M^{(3)} = \frac{1}{(1 - n\chi_0)^4} \left[ \chi_0^{(3)} + \frac{2G^\alpha (\chi_\alpha^{(2)})^2}{1 - G^\alpha \chi_\alpha} + \frac{2G^\mu (\chi_\mu^{(2)})^2}{1 - G^\mu \chi_\mu} \right] \tag{6}$$

where $n$ is the magnetic exchange coefficient. Only the $\alpha$-mode is present for $\boldsymbol{H}$ parallel to [0 0 1]. $\chi_0$ is the anisotropic magnetic susceptibility. For each symmetry, three single-ion susceptibilities are introduced, which are known as soon as the CEF is determined: $\chi_0^{(3)}$ describes the $H^3$-term of the magnetic response in the absence of any interaction. The strain susceptibility, $\chi_\mu = \partial \langle O_2^\mu \rangle / \partial \varepsilon^\mu$, is responsible for the softening of the associated elastic constant:

$$C^\mu = C_0^\mu - \frac{(B^\mu)^2 \chi_\mu}{(1 - K^\mu \chi_\mu)}. \tag{7}$$

$\chi_\mu^{(2)} = \partial \langle O_2^\mu \rangle / \partial H^2$ is the quadrupolar response to a magnetic field and determines the parastriction, which includes the renormalization of the applied field with respect to the bilinear interactions and of the quadrupolar response with respect to the quadrupolar pair interactions:

$$\varepsilon^\mu = \frac{B^\mu}{C_0^\mu} \frac{\chi_\mu^{(2)}}{(1 - G^\mu \chi_\mu)(1 - n\chi_0)^2} H^2. \tag{8}$$

Each of the $\varepsilon^\mu$ can be determined from the combinations of $\lambda_{\alpha_1 \alpha_2 \alpha_3}^{\beta_1 \beta_2 \beta_3}$, relative changes of length induced by a $(\beta_1 \beta_2 \beta_3)$ magnetic field and measured in appropriate $(\alpha_1 \alpha_2 \alpha_3)$ directions. After the determination of the CEF and of the single-ion susceptibilities, the fit of the magnetic susceptibility along the [0 0 1] axis and in the basal plane provides us

with $n$. The other experiments (third-order susceptibility, elastic constant and parastriction measurements) give the different pairs of coefficients $B^{\mu}$ and $K^{\mu}$.

## 3. The crystalline electric field

The knowledge of this coupling is of fundamental importance to using the susceptibility formalism successfully. Indeed, a possible criticism which might be made of previous studies is that the quantum treatment, despite being properly applied for analysing light scattering results and determining the low-lying levels, has been forsaken in favour of less fundamental pseudo-spin methods when it comes to the description of the magnetic and magnetoelastic properties. The continued application of the quantum treatment allows additionally achievement of an understanding of the fundamental couplings, which may then be compared across a series (here $RPO_4$ and $RVO_4$).

Recently, a systematic determination of the CEF in $RPO_4$ has been undertaken using neutron spectroscopy (Loong *et al* 1993a, b, c, Loong and Soderholm 1994). In comparison with that of light scattering, this technique directly provides one with information on the splitting of the Russell–Saunders ground-state multiplet. However, although the neutron spectra are relatively easy to analyse in terms of magnetic dipole matrix elements, the set of the five CEF parameters present in tetragonal symmetry is not unique and the knowledge of the actual solution has required an analysis in close connection with the light scattering data, i.e. considering several multiplets. Quite reliable CEF parameters are now available for $TmPO_4$, $ErPO_4$, $HoPO_4$ and $TbPO_4$. They present a great coherency, although their variation across the series is not especially easy to explain.

Since the susceptibility formalism is used to analyse thermodynamical properties below room temperature, it is developed on the basis of the Stevens equivalent-operators method, i.e. within the hypothesis of zero intermultiplet mixing; the above CEF parameters have then to be slightly modified. Indeed, the direct use of the values from Loong *et al* (1993a) leads to level spacings different by a few per cent (table 1) and thus to thermal variations of the different single-ion susceptibilities not in perfect agreement with the experimental ones. This is particularly easy to check for $TmPO_4$ in the case of the $\chi\delta$-strain susceptibility, which leads to an extremum of the $C_{66}$ elastic constant calculated at 17 K and observed at 21 K by Harley and Manning (1978). Our least-squares procedure starts from the $V_l^m$ of Loong *et al* (1993a) in order to describe the transfers observed using neutron spectroscopy, and searches for minima in the residue in the space of the $V_l^m$. It was fruitfully used for R tetragonal intermetallics, for which neutron spectroscopy is the only possible microscopic technique to apply (Morin and Blanco 1993). Set 2 in table 1 perfectly describes the level scheme for the low-lying levels, and thus the thermal anomalies of the susceptibilities; note however a discrepancy for the high-lying levels, which was already observed by Loong *et al* (1993a). This solution is used in the following sections.

## 4. Samples and experimental techniques

The well-known method of spontaneous crystallization by precipitation from the melt was used to grow the single crystals of $TmPO_4$ with a $PbO–PbF_2–Pb_2P_2O_7–H_3BO_3$ melt as a solvent. The crystals were transparent and slightly coloured, and their average dimensions were about $2 \times 1 \times 1$ mm$^3$ in the directions of the crystallographic axes, the largest one being along the $c$-axis. The crystals were aligned by an x-ray method with an accuracy better than $1^{\circ}$. The magnetization measurements were performed in magnetic fields up to

**Table 1.** Spacings from the ground-state singlet $\Gamma_1$ observed using (a) neutron spectroscopy (Loong *et al* 1993a), (b) light scattering (Becker *et al* 1984) and (c) Raman spectroscopy (Guha 1981) and calculated on the basis of the hypothesis of zero intermultiplet mixing, with the CEF parameters $V_2^0 = 227$ K, $V_4^0 = 40$ K, $V_4^4 = 1003$ K, $V_6^0 = -63$ K, $V_6^4 = 75$ K (set 1) from Loong *et al* (1993a) and with $V_2^0 = 258$ K, $V_4^0 = 47$ K, $V_4^4 = 989$ K, $V_6^0 = -67$ K, $V_6^4 = 60$ K (set 2, present work). The labels in the first line are the ones used by Loong *et al* (1993a).

| $\Delta_{ij}$ (K) | $\Gamma_5^{(2)}$ | $\Gamma_3$ | $\Gamma_5^{(2)}$ | $\Gamma_2$ | $\Gamma_1$ | $\Gamma_4$ | $\Gamma_5^{(2)}$ | $\Gamma_3$ | $\Gamma_4$ |
|---|---|---|---|---|---|---|---|---|---|
| (a) | 41.6 | 112 | 195 | 265 | 352 | 400 | 404 | 517 | 520 |
| (b) | 44.2 | 110 | 208 | | | | | | |
| (c) | 41.8 | 121 | 198.7 | | 403 | | | | |
| Set 1 | 38.5 | 102.6 | 187.2 | 258.1 | 348.5 | 398.1 | 400.6 | 511.4 | 516.5 |
| Set 2 | 41.6 | 112.1 | 195.1 | 265 | 351.4 | 400.6 | 404.4 | 552.8 | 556.9 |

7.6 T in the temperature range 1.5–300 K. The temperature was regulated within $\pm 0.01$ K and the accuracy of the magnetization was around 0.02 $\mu_B$. Magnetostriction data have been collected with strain gauges in fields up to 5 T and in temperatures from 1.5 to 200 K both parallel and perpendicular to the external magnetic field, which pointed along one of the principal symmetry axes of the crystal. The sensitivity is limited to around $2 \times 10^{-7}$ in the liquid-helium temperature range and to $10^{-6}$ at high temperatures. Additional data have also been collected in the case of the $\delta$-symmetry using a capacitance dilatometer in fields up to 0.6 T (du Trémolet de Lacheisserie 1975).

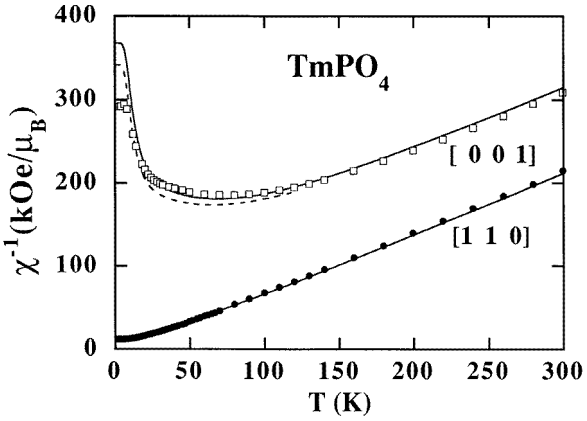


**Figure 1.** Temperature dependences of the reciprocal susceptibility of $TmPO_4$ along the [1 1 0] and [0 0 1] axes. The full lines are calculated in the absence of any magnetic interactions with set 2, the dashed one with set 1 from Loong *et al* (1993a).

## 5. Magnetic susceptibilities

The isothermal magnetization curves were collected along the [0 0 1], [1 0 0] and [1 1 0] directions. The first- and third-order susceptibility values were then deduced from the zero-field extrapolation and the initial slope of plots of $M/H(H^2)$, respectively. Within the

experimental accuracy, the magnetic susceptibility is isotropic in the basal plane as expected for the tetragonal symmetry. A large anisotropy is observed in favour of the basal plane in particular at low temperature. Measurements of the weak signal along the *c*-axis are then delicate and very sensitive to any small misalignment of the field out of the *c*-axis.

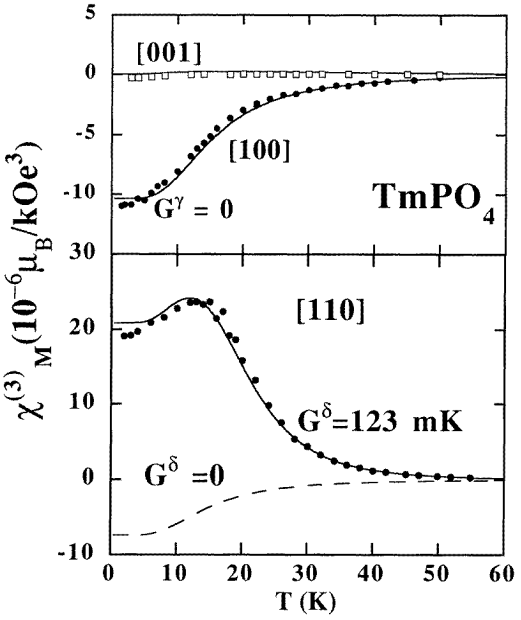


**Figure 2.** Temperature dependences of the third-order susceptibility along the three main crystallographic directions (open squares: data for a field applied along the *c*-axis; full dots: data for a field applied in the basal plane). The curves are calculated for the parameters indicated and in the absence of magnetic and quadrupolar $\alpha$-interactions.

### *5.1. First-order magnetic susceptibility*

The temperature variations of the reciprocal susceptibility are shown in figure 1. At high temperatures, the variation is close to a Curie–Weiss law, with slightly different slopes however along the [0 0 1] and [1 1 0] axes, which indicate CEF effects still present at room temperature; the effective moments differ from the free-ion value by about 5% and 1%, respectively. At low temperature, the Van Vleck behaviour agrees with the non-magnetic nature of the singlet ground state. Set 2 gives a good fit to the data without bilinear interactions ($n = 0$). The slight overestimation of the susceptibility along [0 0 1] below 10 K may be due to a small misorientation.

### *5.2. Third-order magnetic susceptibility*

The temperature dependences of the $\chi_M^{(3)}$ are shown in figure 2. Along the [1 1 0] axis, the $\chi_M^{(3)}$-data are positive in the thermal range investigated, unlike the values calculated without quadrupolar interactions. Quadrupolar interactions characterized by $G^\delta = 123$ mK drive the calculated variation to be positive and close to the experimental one. The contribution (see equation (6)) of quadrupolar interactions within the $\alpha$-symmetry remains negligible. Along the [1 0 0] axis, the third-order susceptibility is negative down to the lowest temperature and is not significantly sensitive to quadrupolar interactions within the $\gamma$-symmetry.

Along the [0 0 1] hard-magnetization axis, the third-order magnetic susceptibility is weakly positive; the maximum value at around 20 K is about $1.5 \times 10^{-8}$ $\mu_B$ kOe$^{-3}$—

that is, two orders of magnitude smaller than along the other two directions. It exhibits an almost zero value at low temperature. Taking into account its weakness and thus the possible parasitic contributions due to misalignments, $\chi_M^{(3)}$ is correctly described by the calculation. To consider quadrupolar $\alpha$-interactions of reasonable magnitude does not improve the fit; as already observed in the basal plane, the quadrupolar $\alpha$-interactions do not appear very active in $TmPO_4$. The Van Vleck behaviour is determined by the wave function of the ground-state singlet, $0.86|0\rangle + 0.36(|4\rangle + |-4\rangle)$, which leads to a very small value of $\chi_M^{(3)}$ (0 K) due to its dominant $|0\rangle$ component. This is fully reminiscent of the third-order susceptibility measured along the $c$-axis in $HoVO_4$ (Morin *et al* 1995).

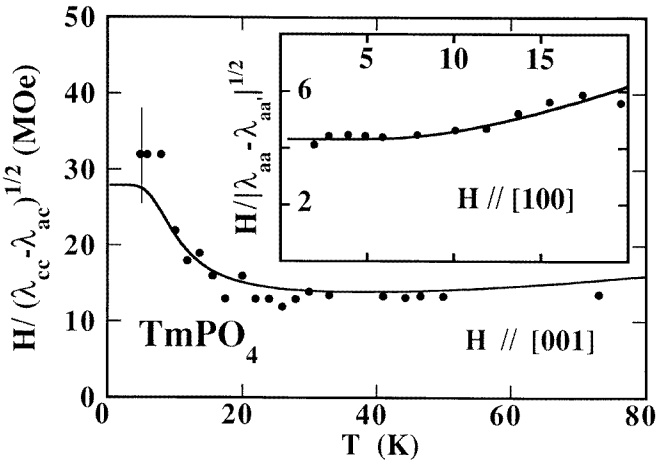


**Figure 3.** Temperature dependences of the parastriction for the $\alpha_2$-mode ($\boldsymbol{H}$ parallel to the [0 0 1] axis; full dots: data); the full line corresponds to the fit using $A^{\alpha 2} = 4.7 \times 10^{-5}$. The inset gives the thermal dependence for the $\gamma$-mode ($\boldsymbol{H}$ parallel to the [1 0 0] axis; full dots: data); the curve is calculated with $B^{\gamma} = 78$ K, $C_0^{\gamma} = 106$ K and $G^{\gamma} = 0$ mK.

## 6. Parastriction measurements

Magnetostriction data have been collected in a magnetic field applied successively parallel to the [1 0 0], [1 1 0], [0 0 1] and [1 0 1] crystallographic directions; gauges were glued along the [1 0 0], [0 1 0] and [0 0 1], [1 1 0] and $[\bar{1}\,1\,0]$, [0 0 1] and [1 0 0], [1 0 1] and $[\bar{1}\,0\,1]$ directions, respectively. Shortened notation for the relative changes of length is used in the following: $\lambda_{ij} = \lambda_{\alpha_1\alpha_2\alpha_3}^{\beta_1\beta_2\beta_3}$. The first subscript, $i$, corresponds to the gauge direction, and the second one, $j$, to the field direction ($i, j = \boldsymbol{a} \equiv [1\,0\,0]$, $\boldsymbol{a}' \equiv [0\,1\,0]$, $\boldsymbol{b} \equiv [1\,1\,0]$, $\boldsymbol{b}' \equiv [\bar{1}\,1\,0]$ and $\boldsymbol{c} \equiv [0\,0\,1]$). Each isothermal variation is plotted against the square of the field. Then the temperature dependence of the initial slope is compared to the predictions from the susceptibility formalism in a linearized form deduced from equation (8).

### *6.1. The $\alpha$-mode*

In a [0 0 1] magnetic field, the changes of length, $\lambda_{cc}$ and $\lambda_{ac}$, lead to the tetragonal symmetry modes $\varepsilon^{\alpha 1} = \lambda_{cc} + 2\lambda_{ac}$ (volume change) and $\varepsilon^{\alpha 2} = \lambda_{cc} - \lambda_{ac}$ (change of $c/a$). For $TmPO_4$ the values are clearly smaller than for $TbPO_4$ and $HoVO_4$, which indicates a small $\chi_{\alpha}^{(2)}$-susceptibility, as observed for the [0 0 1] third-order susceptibility. The accuracy of the

measurements is higher for the $\varepsilon^{\alpha 2}$-mode than for the $\varepsilon^{\alpha 1}$-mode since systematic errors cancel in the difference. The temperature variation of $H/|\lambda_{cc} - \lambda_{ac}|^{1/2}$ is plotted in figure 3. In the absence of bilinear interactions, the calculated behaviour is given by

$$\frac{H}{\sqrt{|\lambda_{cc} - \lambda_{ac}|}} = 4\sqrt{\frac{2}{3}}\frac{1}{\sqrt{|A^{\alpha 2}|}}\frac{1}{\sqrt{|\chi_\alpha^{(2)}|}}(1 - G^\alpha \chi_\alpha)^{1/2}.$$

$A^{\alpha 2}$ depends on both the background elastic constants and the magnetoelastic coefficients, $B^{\alpha 1}$ and $B^{\alpha 2}$:

$$A^{\alpha 2} = \frac{B^{\alpha 2}C_0^{\alpha 1} - B^{\alpha 1}C_0^{\alpha 12}}{C_0^{\alpha 1}C_0^{\alpha 2} - (C_0^{\alpha 12})^2}.$$

The fit to the data leads to $A^{\alpha 2} = 4.7 \times 10^{-5}$. Introducing $G^\alpha$-values in the previous expression is not efficient and confirms the weakness of the $\alpha$-susceptibilities. The $A^{\alpha 2}$-value is exactly opposite to the value determined for $TbPO_4$ (Morin *et al* 1994), which originates from the values of $\alpha_J$ for these two compounds being opposite as discussed later. Assuming opposite values for $A^{\alpha 1}$ also and using the same background elastic constants ($C_0^{\alpha 1} = 24$, $C_0^{\alpha 2} = 11$ and $C_0^{\alpha 12} = 1.6$ in units of $10^5$ K) gives magnetoelastic coefficients, $B^{\alpha 1} = -70$ K and $B^{\alpha 2} = 46$ K, opposite to their values for $TbPO_4$. These lead to the magnetoelastic contribution $G^\alpha_{ME} = 4.4$ mK. As discussed for $TbPO_4$, the existence of a magnetoelastic $\alpha$-coupling acting on the non-zero quadrupolar component $\langle O_2^0 \rangle$, already ordered by the CEF, has to be considered *ab initio* in the diagonalization of the starting Hamiltonian. We have checked that such a value does not significantly change either the single-ion susceptibilities or the fits: unlike in the case of $TbPO_4$, quadrupolar $\alpha$-interactions can be neglected in the following analyses.

### *6.2. The $\gamma$-, $\delta$- and $\varepsilon$-modes*

Owing to the singlet ground state, the orthorhombic $\gamma$- and $\delta$-symmetry modes exhibit a Van Vleck behaviour at low temperature. Over the whole temperature range investigated, $\varepsilon^\gamma = \lambda_{aa} - \lambda_{aa'}$ and $\varepsilon^\delta = \lambda_{bb} - \lambda_{bb'}$ are positive and negative, respectively. Since the quadrupolar-field susceptibilities, $\chi_\mu^{(2)}$, are positive, the magnetoelastic coefficients are of opposite sign. As for the $\alpha$-mode, it is convenient to discuss the field-induced strain using a linearized expression deduced from equation (8). For the $\gamma$-mode (see the inset of figure 3), the fit of the data leads to $B^\gamma = 78$ K for a background elastic constant $C_0^\gamma = 96 \times 10^4$ K. This value is almost opposite to the $TbPO_4$ one ($B^\gamma = -100$ K). Owing to the magnitude of the elastic constant, a relatively small value is then deduced for the magnetoelastic contribution: $G^\gamma_{ME} = 6$ mK. Like the third-order susceptibility, the parastriction does not strongly depend on quadrupolar pair interactions and such a value has no sizeable effect in the description of the parastriction.

For the $\delta$-symmetry mode (figure 4), the high-temperature slope leads to a magnetoelastic coefficient $B^\delta = -151$ K with $C_0^\delta = 18.5 \times 10^4$ K, the background elastic constant also used in section 7. The absolute value of this coefficient is very close to that determined for $TbPO_4$. The corresponding magnetoelastic contribution to the total coefficient $G^\delta$ is $G^\delta_{ME} = 123$ mK. Introducing the $G^\delta$-contribution into the fit leads to a global shift of the calculated variation and to a modification of the low-temperature behaviour towards the data: this is achieved with $G^\delta = 130$ mK, a value in agreement with that determined by third-order susceptibility (123 mK); according to equation (5), it leads to a quadrupolar pair interaction coefficient, $K^\delta$, of almost zero, which is unexpected with pair interactions mediated by acoustic phonons and will be discussed in section 8.

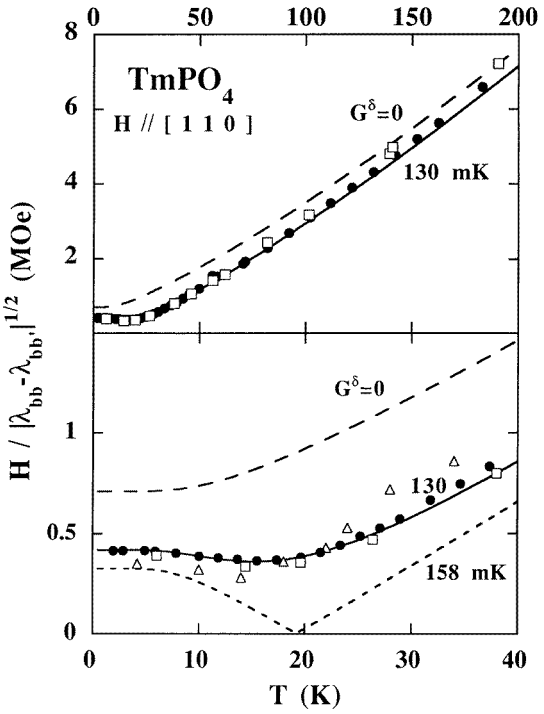


**Figure 4.** Temperature dependences of the $\delta$-symmetry parastriction; upper part: high-temperature behaviour; lower part: low-temperature behaviour. Black dots: strain gauge measurements; open squares: capacitance dilatometer data. The triangles indicate values deduced from Bondar' *et al* (1988) (see the text). The curves are calculated in the absence of magnetic and quadrupolar $\alpha$-interactions with $B^{\delta} = -151$ K, $C_0^{\delta} = 18.5 \times 10^4$ K and the $G^{\delta}$-values indicated.

In particular, the existence of a minimum at around 18 K in the experimental variation of the reciprocal parastriction is described. Its existence was checked by means of strain gauges and capacitance dilatometric measurements with a very good agreement between the two types of experiment; note that it was already present in measurements of the change of length parallel to the field by Bondar' *et al* (1988): data are recalculated here assuming $2\lambda_{bb} = \lambda_{bb} - \lambda_{bb'}$, i.e. neglecting the volume contribution. This minimum moves downwards and becomes more and more pronounced when $G^{\delta}$ increases: it would be zero for the critical $G^{\delta}$-value (about 158 mK) and the quadrupolar component $\langle P_{xy} \rangle$ would order at around 19 K.

The monoclinic mode measured with a field along [1 0 1] is too small to be determined owing to the weak $\varepsilon$-susceptibilities. It is found to be smaller than for $TbPO_4$ ($B^{\varepsilon} = -26$ K).

## 7. Elastic constants

The ultrasonic velocities associated with $C^{\varepsilon} = 2C_{44}$ and $C^{\delta} = 2C_{66}$ were measured by Harley and Manning (1978). $C_{44}$-data were collected from low temperatures up to 150 K and do not reveal sizeable magnetoelastic contributions other than a slight anharmonic lattice behaviour. This agrees with the weakness of the magnetoelastic $\varepsilon$-coupling observed in our parastriction measurements. In contrast, the $\delta$-mode, whose temperature variation

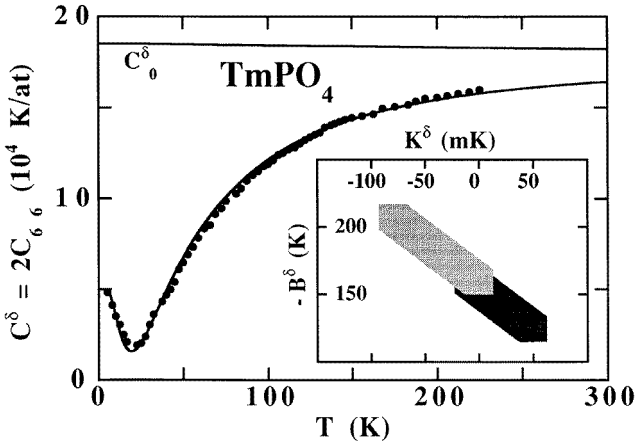


**Figure 5.** Temperature dependences of the $C^\delta = 2C_{66}$ elastic constant; full dots: data from Harley and Manning (1978). $C_0^\delta$ is the lattice background. The full curve is calculated with $|B^\delta| = 162$ K and $K^\delta = -5$ mK. The inset gives the area of possible solutions $(B^\delta, K^\delta)$ deduced from elastic constants and parastriction (dark grey) measurements.

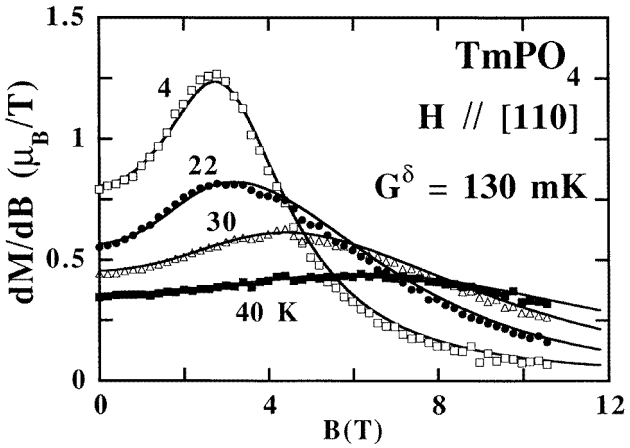


**Figure 6.** Field derivatives of the magnetization measured parallel to the [1 1 0] field for the temperatures indicated; the full lines are calculated with the total quadrupolar coefficient $G^\delta = 130$ mK.

was measured up to 240 K, exhibits, at around 20 K, a pronounced softening of 85% of the high-temperature value, before exhibiting a slight increase towards a low-temperature plateau. This behaviour was very clearly discussed considering the energies of only the low-lying levels. For this reason, the values deduced for the pair interaction and magnetoelastic coefficients were considered as estimates; they led to a ratio $K^\delta/G^\delta_{ME}$ of around $-1/6$. The data were redrawn and are shown in figure 5 and fitted with $|B^\delta| = 162$ K ($G^\delta_{ME} = 142$ mK) and $K^\delta = -5$ mK, i.e. $G^\delta \approx 137$ mK. This pair of quadrupolar coefficients is not unique for describing the ultrasonic data (see the inset of figure 5); it is however compatible with the values fitting the $\delta$-parastriction, and the combined analysis of the two experiments allows us to reduce the area of possible values in the $(B^\delta, K^\delta)$ plane.

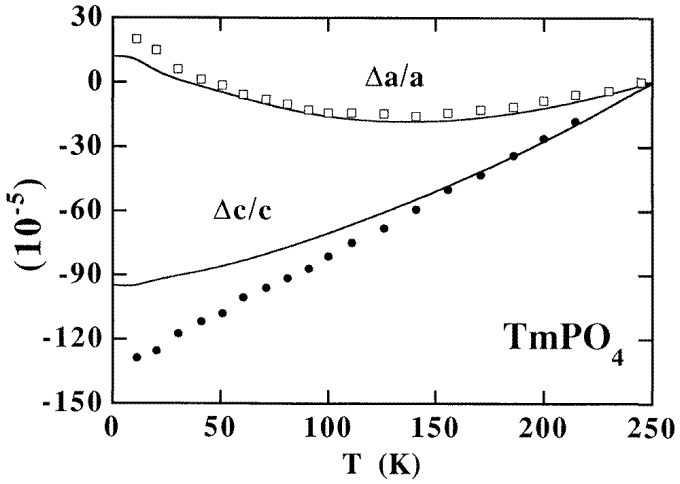


**Figure 7.** Relative changes of the lattice parameters, $\Delta a/a$ and $\Delta c/c$, as functions of temperature. The data are redrawn from Sokolov *et al* (1992). The full lines are calculated using the magnetoelastic $\alpha$-coefficients determined from the magnetostriction and using the lattice behaviour measured by Skanthakumar *et al* (1995a) in $LuPO_4$ (see the text).

## 8. Magnetization

The parameters obtained with the susceptibility formalism allow us to perform calculations for the full magnetization processes. The [1 1 0] magnetization curve was observed to present a more or less pronounced increase at a critical field according to temperature (Ioffe *et al* 1981). Figure 6 gives the field derivative of the isothermal magnetization that we have measured along the [1 1 0] axis. Calculations show that the maximum of the field derivative is associated with an increase of the order parameter $\langle P_{xy} \rangle$ and corresponds to the tetragonal–orthorhombic transition driven by the field of the appropriate symmetry. This feature is reminiscent of the orthorhombic $\gamma$-structure restored at high temperature, above $T_Q$, by the [1 0 0] field in $TmAg_2$ (Morin and Rouchy 1993).

## 9. Discussion

As observed for $TbPO_4$ (Morin *et al* 1994), the magnetoelastic couplings associated with the tetragonal $\alpha$-symmetry (the change of the ratio $c/a$ as well as the change of the volume) are sizeable. The experimental value of $A^{\alpha 2}$ found in section 6.1 and the then-deduced magnetoelastic coefficients $B^{\alpha 1} = -70$ K and $B^{\alpha 2} = 46$ K are opposite in sign to those found for $TbPO_4$. As all of the magnetoelastic coefficients are of one-ion origin, they behave as CEF parameters; in order for us to be able to compare them from one compound to the other, they have to be normalized with respect to the second-order Stevens coefficient, $\alpha_J$, which retains the same value, but changes in sign between $Tb^{3+}$ and $Tm^{3+}$. The values $B^{\alpha 1}/\alpha_J = -6.9 \times 10^3$ K and $B^{\alpha 2}/\alpha_J = 4.6 \times 10^3$ K estimated for $RPO_4$ are also reminiscent of the values obtained for $HoVO_4$ ($-4050$ K and $+6300$ K, respectively). The quite sizeable magnitude of these magnetoelastic $\alpha$-couplings seems to be general for R zircons, in contrast to the case for the tetragonal intermetallics $RAg_2$, for which these values are about 20 or 50 times smaller (Morin and Rouchy 1993).

Additional experimental evidence for their existence can be obtained from the thermal expansion in the absence of any external stress (Morin *et al* 1988). Indeed the magnetic contribution to the lattice parameters is related to the thermal variation of the quadrupolar component $\langle O_2^0 \rangle$:

$$\lambda_c = \Delta c/c = (A^{\alpha 1} + \sqrt{2}A^{\alpha 2})\frac{\langle O_2^0 \rangle}{\sqrt{3}} \qquad \text{and} \qquad \lambda_a = \Delta a/a = \left(A^{\alpha 1} - \frac{1}{\sqrt{2}}A^{\alpha 2}\right)\frac{\langle O_2^0 \rangle}{\sqrt{3}}. \tag{9}$$

X-ray measurements by Sokolov *et al* (1992) have shown that the thermal expansion does not reduce to the lattice behaviour for any of the magnetic $RPO_4$ zircons. This was confirmed via powder neutron diffraction measurements on the system $HoP_{1-x}V_xO_4$ performed by Skanthakumar *et al* (1995b). Using the values $A^{\alpha 2} = 4.7\times10^{-5}$ K and $A^{\alpha 1} = -3.2\times10^{-5}$ K determined from the magnetostriction in $TbPO_4$ and $TmPO_4$ and the lattice behaviour measured for $LuPO_4$ by Skanthakumar *et al* (1995a) one gets the temperature dependence shown in figure 7. The fit to the data obtained without any adjustable parameter is quite promising and motivates us to develop more accurate capacitance measurements of the thermal expansion, in particular for R zircons where the $G^\alpha$-effects are sizeable like in $TbPO_4$ (Morin *et al* 1994).

Indeed, the magnetoelastic $\alpha$-modulation of the CEF leads to an apparent second-order CEF parameter, $\alpha_J V_2^0 - G^\alpha \langle O_2^0 \rangle$, which is temperature dependent and drives a level 'breathing' scheme larger or smaller depending on the spacing and the quadrupolar component $\langle O_2^0 \rangle$ of the low-lying levels. The effects are large for $TbPO_4$, mainly since the spacings from the ground state are small (3.6, 13.7, 29.8 K, ...). In $TmPO_4$, the $\Gamma_1$–$\Gamma_5^{(2)}$ gap of 41 K is increased by only 0.8 K when including the same $G^\alpha = 3$ mK in the diagonalization of the Hamiltonian. The corrective term, $G^\alpha \langle O_2^0 \rangle$, is only 3% of $\alpha_J V_2^0$ at 0 K and decreases to 2% at 100 K.

The $\gamma$-symmetry properties are handicapped by the weakness of the quadrupolar susceptibilities and do not depend sizeably on the $G^\gamma$-value. The magnetoelastic coefficient, $B^\gamma = 78$ K, deduced from the parastriction, leads to $B^\gamma/\alpha_J = 7800$ K, a value coherent with the one, $10^4$ K, previously found for $TbPO_4$. The determination of $B^\gamma/\alpha_J = 13\,500$ K for $HoVO_4$ shows that for this symmetry, as for the $\alpha$-symmetry, $RPO_4$ and $RVO_4$ are governed by similar magnetoelastic couplings. The magnetoelastic contribution, $G^\gamma_{ME} = 6$ mK, deduced from $B^\gamma$, is small due to the large value of $C_0^\gamma$ (five times larger than $C_0^\delta$), and is not able to modify significantly either the parastriction or the third-order susceptibility.

The $\delta$-symmetry is clearly dominant. The determinations of the quadrupolar couplings are coherent for the various experimental probes, as shown by table 2. The ranges of values determined by parastriction and elastic constant techniques are restricted to their overlap zone in the $(B^\delta, K^\delta)$ plane (see figure 5); the value of $B^\delta$ obtained by parastriction obviously depends on the value of the background elastic constant $C_0^\delta$, which is the same in both fits. The third determination via magnetic measurements is in full agreement.

**Table 2.** Quadrupolar coefficients associated with the $\delta$-symmetry determined for $TmPO_4$.

| | $B^\delta$ (K) | $G^\delta_{ME}$ (mK) | $K^\delta$ (mK) | $G^\delta$ (mK) |
|---|---|---|---|---|
| Parastriction | $-151$ | 123 | — | $-130$ |
| $C^\delta = 2C_{66}$ | $162 \pm 5$ | 142 | $-5 \pm 10$ | — |
| $\chi_M^{(3)}$ | — | — | — | 123 |

For this $\delta$-symmetry also, the value $B^\delta/\alpha_J \approx -15\,000$ K is reminiscent of the previous values, $-14\,400$ and $-24\,400$ K found for $TbPO_4$ and $HoVO_4$. The surprising feature is that the pair interaction coefficient $K^\delta$ is here close to zero, as unambiguously proved by the parastriction. Thus for $TmPO_4$, as already observed by Harley and Manning (1978), the $K^\delta$- and $G^\delta_{ME}$-values are not in agreement with the theoretical ratio, $-\frac{1}{3}$, expected in the case of a dominant acoustic phonon contribution. This is leads to a value of $G^\delta = 130$ mK larger than that for $TbPO_4$ (70 mK).

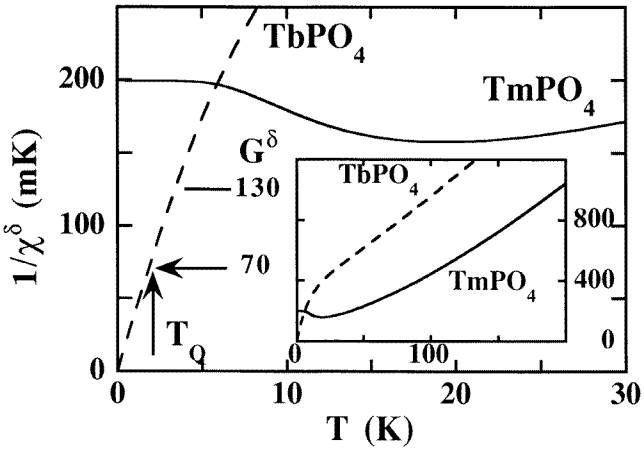


**Figure 8.** Temperature variations of the reciprocal quadrupolar $\delta$-susceptibility of $TmPO_4$ (full lines) and $TbPO_4$ (dashed lines). The value $G^\delta = 70$ mK determined for $TbPO_4$ drives a quadrupolar ordering at 2.2 K, as experimentally observed. The value $G^\delta = 130$ mK is not able to do the same for $TmPO_4$.

The occurrence of the quadrupolar ordering is governed by the CEF level scheme itself, which determines the $\chi^\delta$-susceptibility. The ordering occurs at a $T_Q$-value given by $1/\chi^\delta(T_Q) = G^\delta$. In spite of the small $G^\delta$-value, the $TbPO_4$ system undergoes quadrupolar ordering owing to the nature of the doublet ground state, whereas that of $TmPO_4$ remains undercritical, the critical $G^\delta$-value being at around 158 mK (figure 8). The $1/\chi^\delta$ behaviour observed for $TmPO_4$ is closely reminiscent of that observed for $TbVO_4$, where the quadrupolar interactions are large enough to drive a $\delta$-ordering, the change to the undercritical regime being observed via dilution in the $Tb_xGd_{1-x}VO_4$ system (Harley *et al* 1974). Since $TmPO_4$ is close to criticality, the quadrupolar ordering can be stimulated by external stresses: magnetic fields or uniaxial stresses. The enhancement of the magnetization in [1 1 0] magnetic fields discussed in section 8 is a signature of this effect; an additional one is the sudden increase of the deformation observed at low temperature in fields up to 80 kOe (Kaplan *et al* 1992). The inflexion point of their field dependence corresponds to the structural transition thus induced. As discussed by Vekhter *et al* (1987), an external magnetic field along a non-active JT direction—for instance the [1 0 0] axis here—changes the spectrum and the wave functions in such a way that the quadrupolar $\delta$-transition can occur at a critical field (about 10 T), unfortunately out of the range currently accessible. The verification of this assumption is under way.

The spectroscopic, magnetic and magnetoelastic properties are now described for $TmPO_4$. The magnetoelastic coefficients, coherently determined for the different symmetry-lowering modes by different techniques, are quite comparable with those found for $TbPO_4$

as well as for $HoVO_4$. Thus the occurrence of a Jahn–Teller transition for a given rare-earth zircon essentially depends on the CEF in association with the P, V element. From this comparison, a great coherency among the large family of R zircons can be expected as well as numerous spectacular effects of the interplay between magnetic and magnetoelastic properties, such as the quadrupolar $\delta$-transition assisted by a magnetic field.

## Acknowledgments

The Laboratoire Louis-Néel is a Unité Associée à l'Université Joseph-Fourier, Grenoble. This research was supported, in part, by the Russian Fundamental Science Foundation. One of us, ZK, would like to thank the French Ministère de la Recherche et de la Technologie for its support and the Laboratoire Louis-Néel for its hospitality.

## References

Amara M, Morin P and Burlet P 1995 *Physica* B **210** 157
Becker P C, Hayhurst T, Shalimoff G, Conway J G, Edelstein N, Boatner L A and Abraham M M 1984 *J. Chem. Phys.* **81** 2872
Bondar' I A, Vekhter B G, Kazei Z A, Kaplan M D, Mezentzeva L P and Sokolov V I 1988 *Sov. Phys.–JETP* **68** 1460
Clougherty D P, Johnston K H and McHenry M E 1989 *Physica* C **162–164** 1475
du Trémolet de Lacheisserie E 1970 *Ann. Phys., Paris* **5** 267
——1975 *Revue Phys. Appl.* **10** 169
Elliott R J, Harley R T, Heyes W and Smith S R P 1972 *Proc. R. Soc.* A **238** 217
Gehring G A and Gehring K A 1975 *Rep. Prog. Phys.* **38** 1
Guha S 1981 *Phys. Rev.* B **23** 6790
Harley R T, Hayes W, Perry A M, Smith S R P, Elliott R J and Saville I D 1974 *J. Phys. C: Solid State Phys.* **7** 2145
Harley R T and Manning D I J 1978 *J. Phys. C: Solid State Phys.* **11** L633
Ioffe V A, Andronenko S I, Bondar' I A, Mezentzeva L P, Bazhan A N and Bazan C 1981 *JETP Lett.* **34** 562
Kaplan M D, Kazei Z A, Popov Yu F and Vekhter B G 1992 *Physica* B **182** 53
Knoll K D 1971 *Phys. Status Solidi* b **45** 553
Loong C-K and Soderholm L 1994 *J. Alloys Compounds* **207+208** 153
Loong C-K, Soderholm L, Abraham M M, Boatner L A and Edelstein N M 1993a *J. Chem. Phys.* **98** 4214
Loong C-K, Soderholm L, Goodman G L, Abraham M M and Boatner L A 1993b *Phys. Rev.* B **48** 6124
Loong C-K, Soderholm L, Hammonds J P, Abraham M M, Boatner L A and Edelstein N M 1993c *J. Phys.: Condens. Matter.* **5** 5121
Melcher R L 1976 *Physical Acoustics* vol XII, ed W P Mason and R N Thurston (New York: Academic) p 1
Morin P and Blanco J A 1993 *J. Magn. Magn. Mater.* **119** 59
Morin P and Rouchy J 1993 *Phys. Rev.* **48** 256
Morin P, Rouchy J and Kazei Z 1994 *Phys. Rev.* B **50** 12 625
——1995 *Phys. Rev.* B **51** 15 103
Morin P, Rouchy J and Schmitt D 1988 *Phys. Rev.* B **37** 5401
Morin P and Schmitt D 1990 *Ferromagnetic Materials* vol 5, ed K H J Buschow and E P Wohlfarth (Amsterdam: North-Holland) p 1
Schluter M, Lannoo M, Needels M, Baraff G A and Tománek D 1992 *Phys. Rev. Lett.* **68** 526
Skanthakumar S, Loong C-K, Soderholm L, Nipko J, Richardson J W, Abraham M M and Boatner L A 1995a *J. Alloys Compounds* **225** 595
Skanthakumar S, Loong C-K, Soderholm L, Richardson J W, Abraham M M and Boatner L A 1995b *Phys. Rev.* B **51** 5644
Sokolov V I, Kazei Z A and Kolmakova N P 1992 *Physica* B **176** 101
Stevens K W H 1952 *Proc. Phys. Soc.* A **65** 209
Vekhter B G, Golubev V N and Kaplan M D 1987 *JETP Lett.* **45** 168